Received: 9 June 2024 | Revised: 5 August 2024 | Accepted: 23 August 2024

DOI: 10.1002/pen.26954

RESEARCH ARTICLE

POLYMER ENGINEERING AND SCIENCE WILEY

An experimental and numerical effort on the vibration behavior of additively manufactured recycled polyethylene terephthalate glycol components

Çağın Bolat[1] | Abdulkadir Çebi[1] | Sinan Maraş[2] | Berkay Ergene[3]

[1]Faculty of Engineering and Natural Sciences, Department of Mechanical Engineering, Samsun University, Samsun, Turkey

[2]Faculty of Engineering, Department of Mechanical Engineering, Ondokuzmayıs University, Samsun, Turkey

[3]Technology Faculty, Department of Mechanical Engineering, Pamukkale University, Denizli, Turkey

Correspondence
Çağın Bolat, Faculty of Engineering and Natural Sciences, Department of Mechanical Engineering, Samsun University, 55420 Samsun, Turkey.
Email: cagin.bolat@samsun.edu.tr

Abstract

The importance of recycling engineering components and thus obtaining low-cost production solutions has become prominent in today's world. In this study, the mechanical and dynamic behaviors of three-dimensional-printed recycled polyethylene terephthalate glycol (RePET-G) beams were investigated numerically and experimentally for the first time in the literature. Initially, the governing equations of the beams were determined according to the Bernoulli–Euler beam theory, and these equations were numerically solved using the differential quadrature method and ANSYS program. Subsequently, to validate the accuracy of the numerical models, the obtained natural frequencies were compared with experimental results. It was observed that the numerical results showed good agreement with the experimental results. Finally, the effects of beam length, infill rate, and building direction on the natural frequencies of RePET-G beams were investigated. The outcomes showed that as the beam length changed, natural frequencies were significantly affected. Increasing the infill rate, especially for beams with vertical building direction, from 20% to 100% led to a slight decrease in the natural frequency values of the structure. Moreover, it was found that for beams with an infill rate of 100%, the natural frequency values obtained in the horizontal building direction were higher than those obtained in the vertical building direction.

Highlights

- Printable recycled filaments have great potential for vibration applications.
- Sample length affects the first natural frequency value of RePETG parts.
- Differential quadrature and ANSYS methods can be utilized for the vibration.
- For the 3D-printed samples, rising infill rate causes a natural frequency drop.

KEYWORDS
additive manufacturing, natural frequency, numerical analyses, recycling, vibration

1 | INTRODUCTION

Additive manufacturing (AM), also known as three-dimensional (3D) printing, excels in swiftly creating intricate objects when compared to traditional manufacturing methods like machining, forging, welding, and powder sintering. It fabricates components directly from computer-aided design (CAD) models thanks to special computer-aided manufacturing (CAM) programs known as slicing software.[1] Although the target material portfolio of this technology is considerably versatile, from plastics to metals, ceramics, and composites, polymer materials are frequently utilized in active 3D printing applications compared to the others. The easy printability of the thermoplastics, the low melting point of the used filaments, and the cheapness of the raw materials are the most determining factors for this trend. The prevalent materials employed in 3D printing encompass acrylonitrile butadiene styrene (ABS), polycarbonate (PC), nylon 6 (PA6), polylactic acid (PLA), and polyethylene terephthalate glycol (PET-G).[2] There is a growing need to expand the research scope concerning polymer matrix-reinforced composites. Consequently, there has been a recent surge in research in this area. Specifically, investigations have been conducted to examine the influence of fused deposition modeling (FDM) parameters on mechanical properties, with a comprehensive review being undertaken. Parameters can be categorized into three groups: slicing parameters, building direction, and melting temperature requirements. These parameters collectively impact chain bonding and void structure in the rigid body, consequently influencing mechanical properties.[3] Liu et al.[4] suggest that research primarily emphasizes two main aspects: firstly, optimizing key process parameters to enhance bonding and, subsequently, improving mechanical properties. Chacón et al.[5] selected building direction, layer thickness, and feed rate as parameters to investigate their effects on the mechanical properties of PLA samples. Torrado and Roberson[6] opted to examine the impact of different geometries conforming to ASTM standards, building directions, and raster patterns. Parandoush and Lin[7] conducted an exhaustive examination of polymer fiber composites, outlining the challenges encountered in 3D printing. These challenges included printer head blockage, lack of adhesion between fibers and the matrix, extended curing times, agglomerate formation, and the formation of heterogeneous composites. Addressing these issues is crucial, especially in polymer composites featuring discontinuous fibers.

Upon doing an extensive analysis of the literature pertaining to 3D printing of PET-G material, it becomes evident that the majority of studies carried out have focused on examining the impact of fused filament fabrication (FFF) printing settings on the mechanical properties of the resulting components. For example, Srinivasan et al.[8] looked at research on the influence of FFF process parameters on the mechanical characteristics of PET-G and found that raising the infill rate and decreasing layer thickness enhanced the tensile strength. Additionally, Durgashyam et al.[9] conducted research on the effect of various process variables, including infill rate and layer thickness, on the flexural and tensile strength of 3D-printed PET-G components. Their findings indicated that the combination of the thinnest layer thickness and the highest infill rate led to the highest tensile strength. Conversely, the thinnest layer thickness combined with a lower infill rate resulted in superior flexural properties. Moreover, Szykiedans et al.[10] concentrated on the 3D-printed PET-G components' elastic modulus and tensile strength. They found that the differences in Young's modulus values are due to the presence of air gaps in the print structure and stress concentration along the filament beads. According to Ajay Kumar et al.,[11] layer height and infill rate significantly changed the flexural strength of PET-G items made of carbon fiber.

It is known that functional parts produced by AM are used especially in the automotive and aerospace fields, and these parts are exposed to different levels of vibration due to external factors. In order to prevent a possible resonance situation, it is extremely important to determine the natural frequencies of the parts used in advance. As for the dynamic characteristics, the studies listed below provide a summary of how changes in process parameters affect the target outputs. Kam et al.[12] examined how the vibrations from the 3D printer system affected the mechanical characteristics of the printed items. Vibration amplitudes were examined across various orientations and processing speeds to comprehend their impact on the mechanical properties. At this point, PET-G served as the material for printing test samples. Singh et al.[13] analyzed the fluctuations in the complex modulus of the materials to anticipate alterations in the vibration attributes (natural frequencies and damping) of printed constructions based on printing orientation. PLA beams were printed in four distinct orientations, and a dynamic

mechanical analysis device was employed to assess their mechanical properties. Using curve fitting techniques, they approximated the frequency and temperature-dependent complex modulus. These complex moduli were subsequently employed to project the eigenvalues of a standardized beam. They illustrated how printing direction influenced the vibration characteristics (natural frequencies and mode shapes) of a 3D printed beam. Wang et al.[14] manufactured the newly developed 3D Kagome truss with face sheet using selective laser sintering technology and selected thermosetting polyurethane as the viscoelastic filling material. They utilized a novel complex modal analysis finite element method for the hybrid composite lattice truss sandwich. They suggested that the proposed method could provide high stiffness at low mass, significant vibrational performance at low cost, and could be considered as a general vibration design method in lattice truss manufacturing. Lesage et al.[15] investigated the effect of printing orientation on the dynamic response of metallic samples produced by selective laser melting process. The influence of printing orientation on the accelerations, natural frequencies, damping effects, energy absorption, dynamic behaviors, and differences of each sample were examined. A torsional mechanism incorporating multiple rotating disks supported by beams, with a long, thin rod supported vertically, has been designed and fabricated using PET-G through 3D printing to demonstrate the fundamentals of single-degree-of-freedom and two-degree-of-freedom free vibrations of rotational systems. Tekes[16] designed and fabricated a torsional mechanism using PET-G through 3D printing, incorporating multiple rotating disks supported by beams with a long, thin rod supported vertically, to demonstrate the fundamentals of single-degree-of-freedom and two-degree-of-freedom free vibrations of rotational systems. Zolfagharian et al.[17] have investigated the control of low-frequency vibration isolation in cylindrical metamaterials through the control of global buckling. The research team has designed the cylinders for 3D printing and conducted finite element analyses and experimental studies to demonstrate their contributions. Zou et al.[18] conducted a study on the vibrational reactions of a delta 3D printer while it was printing, employing data collection and analysis techniques. Their investigation encompassed analyses in both the time and frequency domains, through which they established the relationship between vibration signals and the printing parameters. Kam et al.[19] experimentally dig out the damping capabilities of metal/polymer composite bearings printed using FDM. Zhang et al.[20] performed vibration analysis of a satellite structure composed of lattice sandwich panels fabricated through 3D printing. The results of the vibration tests have demonstrated that the satellite structure can withstand the vibration loads associated with rocket launches. Guo et al.[21] experimentally and numerically analyzed the vibration of a sandwich beam with an hourglass lattice core produced using 3D printing technology.

The governing equation of the beam was formulated using a homogenized model and Hamilton's principle for determining the natural frequencies. To passively suppress the vibration of the sandwich beam, they proposed the use of a nonlinear energy sink (NES). Parpala et al.[22] carried out experimental endeavors on the influence of infill-related parameters on the vibration of 3D-printed samples and proposed a corresponding parametric finite element (FE) model for predicting the natural frequencies of prints. They conducted tests on 3D-printed PLA cantilever beams with different infill rates, perimeter counts, and infill thicknesses to determine their natural frequencies. To assess the impact of the considered infill parameters set on the natural frequencies, the researchers developed a script-based FE model using ANSYS and SpaceClaim software and validated it against experimental outcomes. They determined a weight-frequency response function and additionally used it to predict the first natural frequency of the other three prints with different parameters (pattern type, infill rate, contour/perimeter count). Gunasegeran and Edwin Sudhagar[23] have performed both experimental and numerical efforts into the free and forced vibration analysis of sandwich beams featuring a viscoelastic core inspired by bamboo, which is derived from bioinspired principles. The sandwich beam was subjected to a parametric analysis, exploring four distinct 3D printed bioinspired PLA cores and various ply configurations of the glass fiber/epoxy skin, employing the Higher-Order Shear Deformation Theory (HSDT). Medel et al.[24] have analyzed diverse measurements derived from Laser Doppler Vibrometry (LDV) assessment of 3D printed rectangular prisms and explored the reflexions of different parameters, including structure orientation, scanning angle, nozzle temperature, printing speed, and layer height, on the inherent frequencies and damping coefficients of the specimens. Mizukami and Kumamoto[25] have studied the composite sandwich metamaterials with spiral resonators to mitigate low-frequency structural vibrations. Monkova et al.[26] studied how the mechanical vibration damping and compression properties of a body-centered cubic (BCC) lattice structure, composed of ABS plastic, are affected by the cell size and volume fraction. They tested 3D-printed ABS samples to scrutinize their vibration damping characteristics when subjected to harmonic excitation with three inertial masses. The experimental findings indicated that as the volume ratio (or specimen stiffness) decreased and the cell size (or specimen

thickness) increased, the mechanical vibration damping capability of the examined 3D-printed ABS plastic lattice structures improved. Carter et al.[27] delved the vibration properties of 3D printed axially graded viscoelastic gradient polymer plates. Ergene et al.[28] examined how 3D printing parameters, including layer heights (0.1 mm, 0.2 mm, and 0.4 mm), infill rates (40%, 70%, and 100%), and geometric characteristics like tapered angle variations (0, 0.25, and 0.50), affect the vibrational characteristics of PET-G tapered beams produced through FFF. Their findings indicate that higher infill rates lead to higher natural frequencies, whereas an increase in the taper angle from 0 to 0.25 causes a decrease in natural frequency values. Carter[29] conducted both experimental and numerical studies to comprehend the vibration and aeroelastic response traits of 3D-printed structures, which were graded using multiple viscoelastic polymer materials. Their research illustrated the influence of grading patterns and distributed material properties on various aspects of vibration, such as mode shape, frequency, damping, and on the aeroelastic performance, particularly flutter, of such structures. Mahesh[30] conducted experimental studies to examine the natural frequencies and mode shapes of PET-G-based composites reinforced with short carbon fibers (CF) and organically modified montmorillonite (OMMT) nanoclay (NC) produced using AM. Their findings indicated that the experimental outcomes underscored the notable impact of both boundary conditions and the weight percentages of reinforcements on establishing the frequency and damping parameters of the PET-G composite beam. Mansour et al.[31] demonstrated the mechanical and dynamic properties of FFF-printed PET-G and PET-G reinforced with 20% carbon fibers using a range of experimental tests. The loss factor and damping, determined from the cyclic compression and modeling tests, decreased from 17.3% to 15.4% and from 13.8% to 12.3%, respectively. Kannan et al.[32] examined the vibration and bending characteristics of 3D printed carbon fiber reinforced PLA composite beams via the first-order shear deformation theory (FSDT) and the FE method. Additionally, they experimentally obtained the natural frequencies of carbon fiber reinforced and unreinforced 3D printed composite beams under different boundary conditions. They parametrically evaluated the effect of aspect ratio and boundary conditions on the vibration and bending responses of 3D-printed composites. According to the analysis findings, it was found that CF-reinforced PLA demonstrated a 25% rise in elastic modulus when compared to pure PLA lacking CF reinforcement, along with a 17% increase in natural frequencies. It has been observed that as the aspect ratio increases, the natural frequencies decrease. Through modal analysis and experimental design, Xue et al.[33] probed how four process parameters (raster angle, nozzle temperature, layer height, and deposition speed) shift the vibration properties of advances in FFF-printed PLA structures. It was determined that the raster angle was the most significant factor on both the resonance frequency (by 16.6%) and the damping factor (by 7.5%). Senthamaraikannan et al.[34] investigated the free vibration analysis and mechanical behavior of 3D printed composite I-shaped beams consisting of short carbon fiber-reinforced ABS and PLA materials. They noted that ABS-based beams exhibited superior stiffness and damping characteristics compared to PLA-based versions.

When examining the published studies on 3D printed beams produced by FFF in the literature, it is observed that mechanical tests such as bending, compression, tension, energy absorption, and low-velocity impact behaviors of these structures are generally conducted. Herein, the majority of the studies are experimental. Despite studies on the mechanical and dynamic properties of 3D printed beams, there are few studies that simultaneously investigate the experimental and numerical dynamic properties of these structures. On the other side, the global interest in environmental friendliness, clean manufacturing, and green materials has escalated day by day. Right at this point, the importance of recycling the engineering components comes to the forefront, thereby obtaining low-cost manufacturing solutions. Within this scope, to find out their vibration properties, low-cost recycled PET-G (RePET-G) filaments were also tried in this paper for the first time in the literature. To the best of the authors' knowledge, the experimental approach for the free vibration behavior of RePET-G beams, as well as the numerical method of differential quadrature methods (DQM) and its effects on these materials, is completely new and has not been published elsewhere. Concordantly, the effects of three different beam lengths (150, 175, and 200 mm), infill rates (20%, 60%, and 100%), and different building directions (vertical and horizontal) on the free vibration behavior of RePET-G beams were investigated experimentally and numerically using DQM and the FE software ANSYS. A pulse vibration test system and Dewesoft X data acquisition and signal processing software were used for the experimental measurement of the beams' vibration properties.

2 | MATERIALS AND METHODS

2.1 | Material, 3D printing, and testing procedure

The RePET-G filament was supplied by Porima Polymer Technology A.Ş. (Yalova, Türkiye). The technical information provided by the supplier is given as filament color

black, diameter 1.75 mm, nozzle temperature from 230 to 260°C, and bed temperature between 70 and 100°C.

In order to determine the mechanical properties of the filament, a 3D model was designed in the CAD program (SolidWorks 2020®) in accordance with the american society for testing and materials (ASTM) D638-Type 4 standard. Prior to transferring the CAD model data into the Flashprint 5.0 (Flashforge, China) slicing program, the solid model was converted to the "stl" extension. The g-codes required for 3D printing were generated by the Flashprint 5.0 program. The tensile test specimens were produced at different infill rates (20%, 60%, and 100%) by the Flashforge Creator 3 3D printer (Zhejiang Flashforge 3D Technology Co. Ltd., China). The 3D printer has a 0.4 mm hardened nozzle with self-hotend. The nozzle temperature can be up to 300°C as an upper limit. Similarly, the bed temperature can reach a maximum of 120°C. The printing speed can be adjusted from 10 to 150 mm/s. Moreover, the average humidity level of ambient and unwanted air flows, which are crucial phenomenon to the product process of recycled parts, are prevented due to the closed cabinet of the printer. The details of FDM process procedures of tensile test specimens are shown in Table 1. The tensile test specimens were produced horizontally and vertically by rotating 90° on the *x* axis.

Tensile tests were carried out on BMT-300E servo electro-mechanical universal testing machine (Beskom Electronic, Besmak, Türkiye). This machine has a 300 kN load capacity. Also, the machine has 24 bit load measurement resolution and high precision load measurement (0.5 sensitive load cell class). The crosshead moving speed range is from 0.001 to 500 mm/min. All tests were performed at a tensile speed of 5 mm/min. The dimensions of the specimens were measured before the test. The engineering stress and engineering strain data were calculated after gathering the force/stroke data.

Since the tensile test results gave the desired mechanical properties, beams with different lengths were designed in SolidWorks as the second stage. Similarly, the transfer and printing process as above-mentioned was followed in the production of the tensile test specimens. The specimen lengths were determined as 150, 175, and 200 mm. Figure 1 illustrates the 3D printing stages as a slicing program, printing system, and produced the specimens.

In order to detect possible production and dimensional defects that can be encountered in recycled parts, visual inspection, caliper measurement, and weight measurements were performed. The specimen weights were measured by an electronic scale with 0.01-g precision (YP20002, Swock). Six different points were selected in the RePET-G sample geometry to analyze the dimensional changes in width (A_1, A_2, and A_3) and thickness (B_1, B_2, and B_3) values. These points on the beam samples can be monitored in Figure 2.

TABLE 1 The fused deposition modeling process parameters for recycled polyethylene terephthalate glycol (RePET-G) filament.

Parameter	RePET-G
Infill rate (%)	20; 60; 100
Building direction	Vertical and horizontal
Infill pattern	Line
Raster angle (°)	90
Print speed (mm/s)	60
Fan speed (%)	50
Layer height (mm)	0.27
Raft (mm)	1

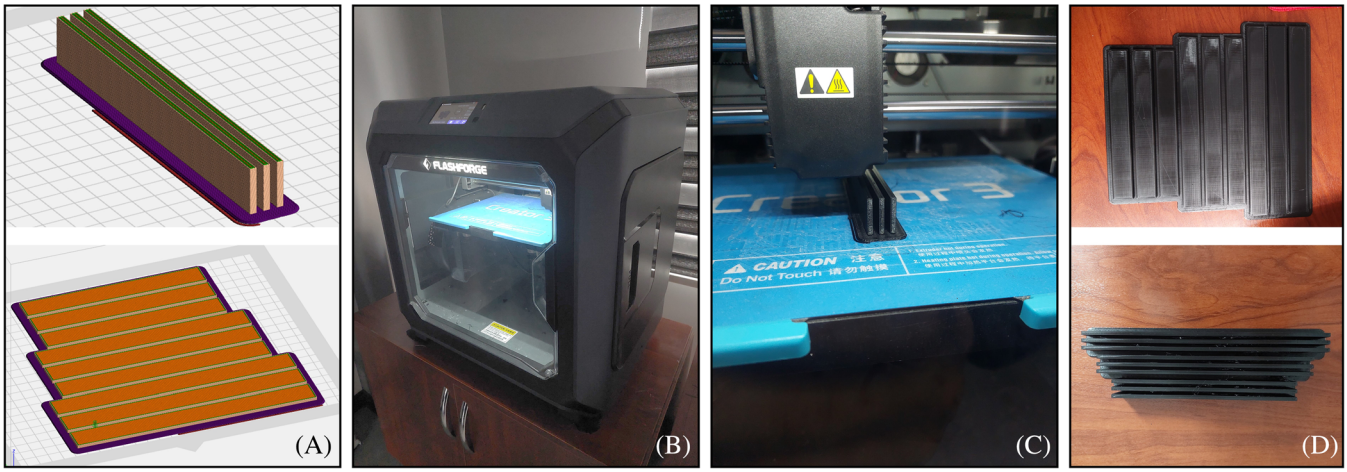

FIGURE 1 The three-dimensional (3D) printing stage (A) slicing program, (B) 3D printer, (C) the printing system, and (D) horizontal and vertical recycled polyethylene terephthalate glycol beams.

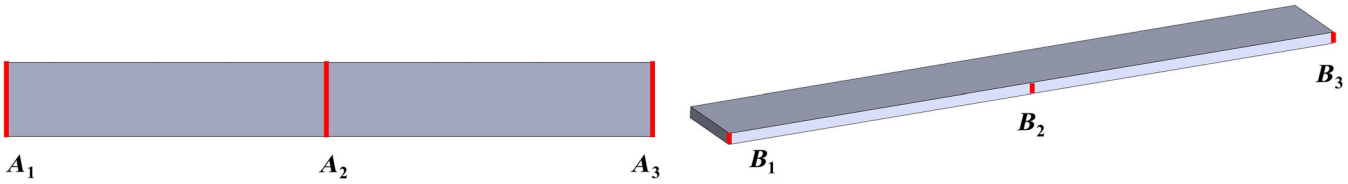

FIGURE 2 The measurement points on the recycled polyethylene terephthalate glycol beam.

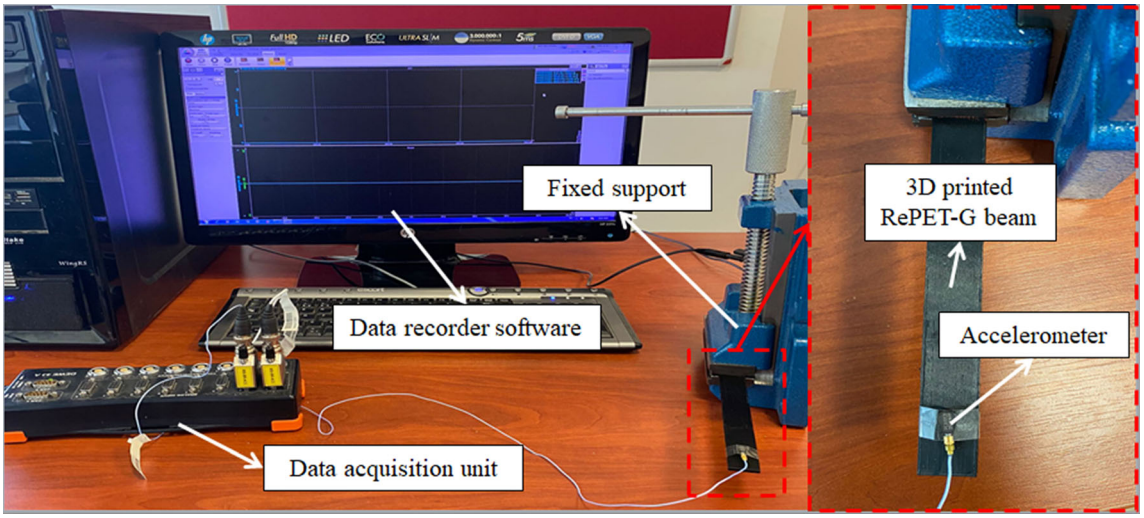

FIGURE 3 An illustration of the experimental vibration set-up. 3D, three-dimensional; RePET-G, recycled polyethylene terephthalate glycol.

To ascertain the vibration behavior of 3D printed RePET-G beams with varying lengths and infill rates, an experimental analysis was conducted using a DEWE-43A universal serial bus (USB) data acquisition system with a channel count of 8, a sampling rate of 200 kS/s, and an operating temperature range of −20 to 60°C. Moreover, during the vibration analysis, the 3D printed RePET-G beams were fixed from one edge, covering a length of 20 mm from the end, while the opposite edge was kept free. Furthermore, a lightweight (0.5 g) accelerometer (PCB35C22) with a frequency range of 1–10,000 Hz and a sensitivity of 10 mV/g was placed on the 3D-printed beam, as shown in Figure 3.

2.2 | Differential quadrature method

The DQM represents the partial derivative of a function concerning a spatial variable at a specified discrete point by expressing it as a weighted linear combination of the function values across all discrete points within the domain of that variable.[35] For instance, when examining the initial derivative of a one-dimensional function $u(x)$ at N discrete points (where $i = 1, 2, ..., N$), the first derivative at the i-th discrete point can be articulated as such:

$$u_x(x_i) = \left.\frac{\partial u}{\partial x}\right|_{x=x_i} = \sum_{j=1}^{N} c_{ij}^{(1)} u(x_j);\ i = 1,2,...,N. \quad (1)$$

Here, x_j represents the discrete points in the variable domain, $u(x_j)$ denotes the function values at these points, and $c_{ij}^{(1)}$ represents the weight coefficients linking these values to the function values for the first derivative. The weight coefficients are calculated using functional approximations in the corresponding coordinate directions. Bellman and Casti[36] obtain the following expression for the calculation of weight coefficients using a test function chosen as a polynomial function of degree $(N-1)$ or lower.

$$u_k(x) = x^{k-1},\ k = 1,2,...,N. \quad (2)$$

When the expression above is inserted into Equation (1), it results in a set of linear equations, as described in Equation (3), for deriving the first-order weight coefficients.

$$(k-1)x_i^{k-2}=\sum_{j=1}^{N}c_{ij}^{(1)}x_j^{k-1}\quad i=1,2,...,N \text{ and } k=1,2,...,N. \tag{3}$$

Similar to the procedures described above, expressions for second- or higher-order derivatives can also be written in the same manner.

If the method for the second derivative is written, the following expression is obtained:

$$u_{xx}(x_i)=\left.\frac{\partial^2 u}{\partial x^2}\right|_{x=x_i}=\sum_{j=1}^{N}c_{ij}^{(2)}u(x_j),\quad i=1,2,...,N. \tag{4}$$

Here, $c_{ij}^{(2)}$ represents the weight coefficients for the second derivative.

When the given polynomial function is applied in Equation (2), the expression for the second derivative becomes as follows:

$$(k-1)(k-2)x_i^{k-3}=\sum_{j=1}^{N}c_{ij}^{(2)}x_j^{k-1} \tag{5}$$

Equation (5) is solved similarly to its relationship in Equation (3). The second, third, and fourth-order weight coefficients $c_{ij}^{(2)}$, $c_{ij}^{(3)}$, and $c_{ij}^{(4)}$ are, respectively, as follows.

$$c_{ij}^{(2)}=\sum_{k=1}^{N}c_{ik}^{(1)}c_{kj}^{(1)}. \tag{6}$$

$$c_{ij}^{(3)}=\sum_{k=1}^{N}c_{ik}^{(1)}c_{kj}^{(2)}. \tag{7}$$

$$c_{ij}^{(4)}=\sum_{k=1}^{N}c_{ik}^{(1)}c_{kj}^{(3)}. \tag{8}$$

Numerous methods exist for choosing node points, with the most prevalent being equally spaced points in every coordinate direction. The equations defining node point selection for both x and y coordinates are as follows:

$$X_i=\frac{i-1}{N_x-1},\quad i=1,2,...,N_x. \tag{9}$$

$$Y_j=\frac{j-1}{N_y-1},\quad i=1,2,...,N_y. \tag{10}$$

2.3 | Linear bending vibration analysis of RePET-G beam with DQM

The governing equation for a Bernoulli–Euler beam under bending is as follows[37]:

$$\frac{\partial^2}{\partial x^2}\left[\mathrm{EI}\frac{\partial^2 w}{\partial x^2}\right]+\rho A\frac{\partial^2 w}{\partial t^2}=0,\quad 0<x<L, \tag{11}$$

where EI denotes the flexural rigidity of the beam, ρA refers to the mass per unit length, and L represents the beam's length.

In the context of free vibration, the transverse displacement w is typically assumed to be:

$$w(x,t)=W(x)e^{i\omega t}. \tag{12}$$

When Equation (12) is inserted into Equation (11) and the equation is subsequently normalized, it results in:

$$\frac{\partial^2 s(X)}{\partial X^2}\frac{\partial^2 W}{\partial X^2}+2\frac{\partial s(X)}{\partial X}\frac{\partial^3 W}{\partial X^3}+s(X)\frac{\partial^4 W}{\partial X^4}=\overline{\omega}^2 W \tag{13}$$

where $s(X)=EI/EI_0, \overline{\omega}^2=(\rho AL^4/EI_0)\omega^2$ and $X=x/L$.

By considering the number of grid points N as shown in Figure 1 and employing the differential quadrature approximation (Equations 11–13) at every discrete point on the grid, one can derive:

$$\begin{aligned}\frac{\partial^2 s(X_i)}{\partial X^2}\left(\sum_{j=1}^{N}c_{ij}^{(2)}W_j\right)+2\frac{\partial s(X_i)}{\partial X}\left(\sum_{j=1}^{N}c_{ij}^{(3)}W_j\right)\\ +s(X_i)\left(\sum_{j=1}^{N}c_{ij}^{(4)}W_j\right)=\overline{\omega}^2 W_i\end{aligned} \tag{14}$$

for $i=1, 2, 3, ..., N$. Equation (14) forms an eigenvalue problem. By solving this eigenvalue problem alongside suitable boundary conditions, the natural frequencies of the structure can be determined.

Let's consider a beam with its left end fixed and its right end free. In this scenario, the boundary conditions are as follows:

$$\begin{aligned}&W=\frac{\partial W}{\partial X}\ \text{ at }\ X=0,\\ &\frac{\mathrm{EI}\partial^2 W}{\partial x^2}=0,\left(\frac{\partial}{\partial x}\right)\left(\frac{\mathrm{EI}\partial^2 W}{\partial x^2}\right)=0\ \text{ at }\ x=\mathrm{L}\end{aligned} \tag{15}$$

or

$$\frac{s(X)\partial^2 W}{\partial X^2}=0,\left\{\frac{\partial s(X)}{\partial X}\right\}\frac{\partial^2 W}{\partial X^2}+\frac{s(X)\partial^3 W}{\partial X^3}=0 \quad \text{at} \quad X=1. \tag{16}$$

Using the differential quadrature approximation (Equation 1) on the boundary conditions (Equations 15 and 16) results in:

$$W_1=0,\ \sum_{j=1}^{N} c_{ij}^{(1)} W_{j=0}. \tag{17}$$

$$s(X_N)\left(\sum_{j=1}^{N} c_{Nj}^{(2)} W_j\right)=0,\ \left\{\partial s\left(\frac{X_N}{\partial X}\right)\right\}\left(\sum_{j=1}^{N} c_{Nj}^{(2)} W_j\right)+s(X_N)\left(\sum_{j=1}^{N} c_{Nj}^{(3)} W_j\right)=0. \tag{18}$$

To incorporate the boundary conditions into Equations (14), (17) and (18) are first used to express W_1, W_2, W_{N-1}, and W_N in terms of the variables W_3, W_4, ..., W_{N-2}. These expressions for W_1, W_2, W_{N-1}, and W_N are then substituted back into Equation (14) to eliminate W_1, W_2, W_{N-1}, and W_N. As a result, only the discretized equations at the points $i = 3, 4, ..., N-2$ are retained in Equation (14). Finally, by solving the remaining eigenvalue problem, the natural frequencies of the structure are obtained.[37]

2.4 | Vibration analysis of RePET-G beam with ANSYS

The vibration analysis of RePET-G beams was conducted using the finite element method with the ANSYS software package. The model was created and analyzed in ANSYS using the SHELL 281 element (Figure 4). The SHELL 281 element features eight nodes, each with six-degrees-of-freedom (translations and rotations in the x, y, and z directions), and has a geometry suitable for analyzing thin shell structures. The material properties obtained from the tensile tests were defined as inputs in the software package. The beam was modeled as structural → linear → elastic → isotropic material. The model consists of 320 elements and 1050 nodes. The ANSYS model of a sample RePET-G beam is shown in Figure 5. The natural frequencies of the structure were numerically obtained through modal analysis performed on the created finite element model.

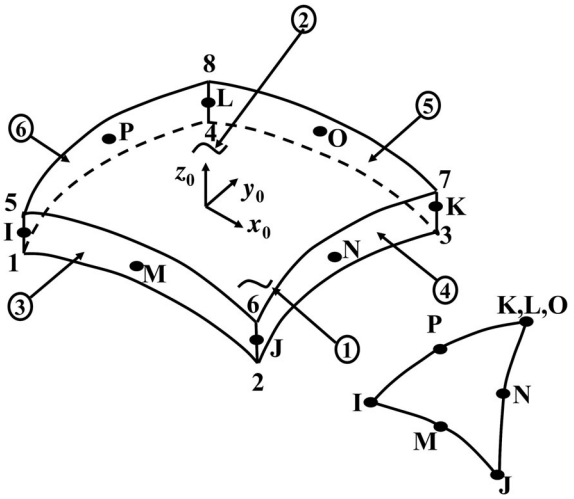

FIGURE 4 The geometry of the SHELL 281 element.[38]

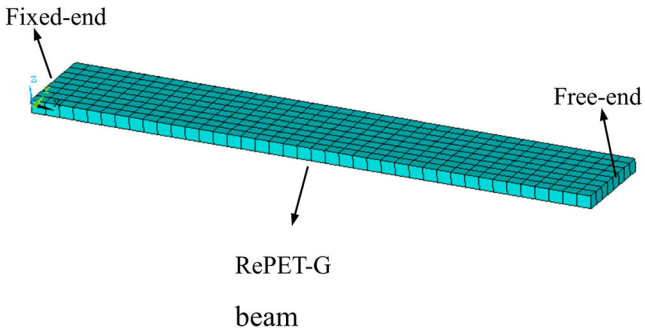

FIGURE 5 The ANSYS model of the recycled polyethylene terephthalate glycol (RePET-G) beam.

3 | RESULTS AND DISCUSSION

3.1 | Physical and mechanical properties

Prior to the vibration analyses, physical evaluations to detect the density values of the RePET-G beams and mechanical properties were probed by applying tensile tests. For the calculation of the density measurement that were also utilized in the numerical efforts in the vibration works, dimensional and weight measurements were carried out to obtain the mass-to-volume ratio of the samples. In light of the measured data, all geometrical outcomes and density alterations according to the production parameters can be followed in Table S1 and Figure 6.

Density values of the produced samples reflected different values depending on the infill rate as a result of

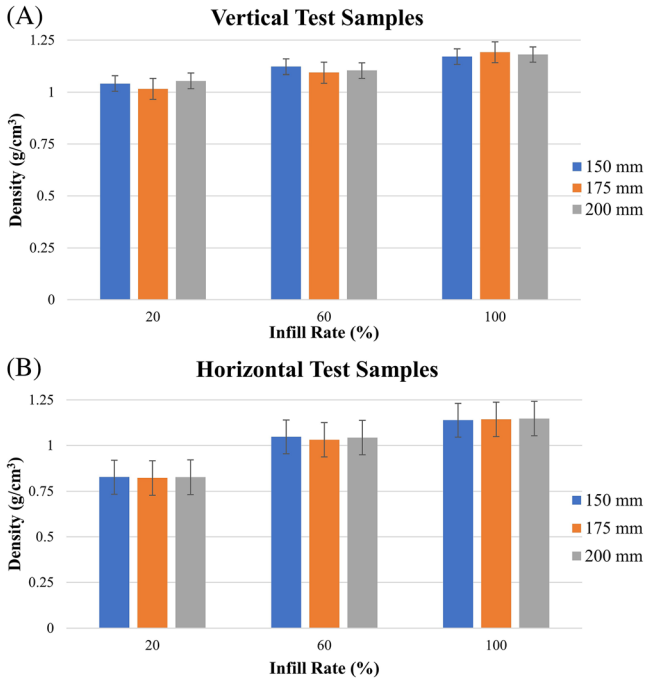

FIGURE 6 Average density values of recycled polyethylene terephthalate glycol beams in various configurations: (A) vertical test samples, (B) horizontal test samples.

the changing production-based gap volume fraction. The lowest average density of 0.8219 g/cm^3 belonged to the horizontally printed sample having a 20% infill rate, whereas the highest value of 1.1914 g/cm^3 was recorded for the vertically printed sample with 100% infill. Based on previous literature,[9,39] the results are compatible with the levels shared for the standard PET-G filament, typically 1.23–1.3 g/cm^3 density. In this article, production gaps between the layers are responsible for the lower density recorded for the 100% infill-rated samples. On the other side, vertically printed samples generally showed higher density values in the same parameter matching compared to their horizontal versions. This case stems from the better stacking capacity of the vertical samples that were accumulated in the thin cross-sectional area with more stacking layer numbers in the direction of gravity.

Figure 7 given below illustrates the engineering stress and engineering strain curves of the produced RePET-G samples according to the tensile tests that were conducted according to ASTM D-638. Looking at the results, it was seen that there was a positive relationship between the infill rate and the mechanical features like tensile

FIGURE 7 Engineering stress/engineering strain curves of the tested samples.
(A) Horizontal test samples.
(B) Vertical test samples.

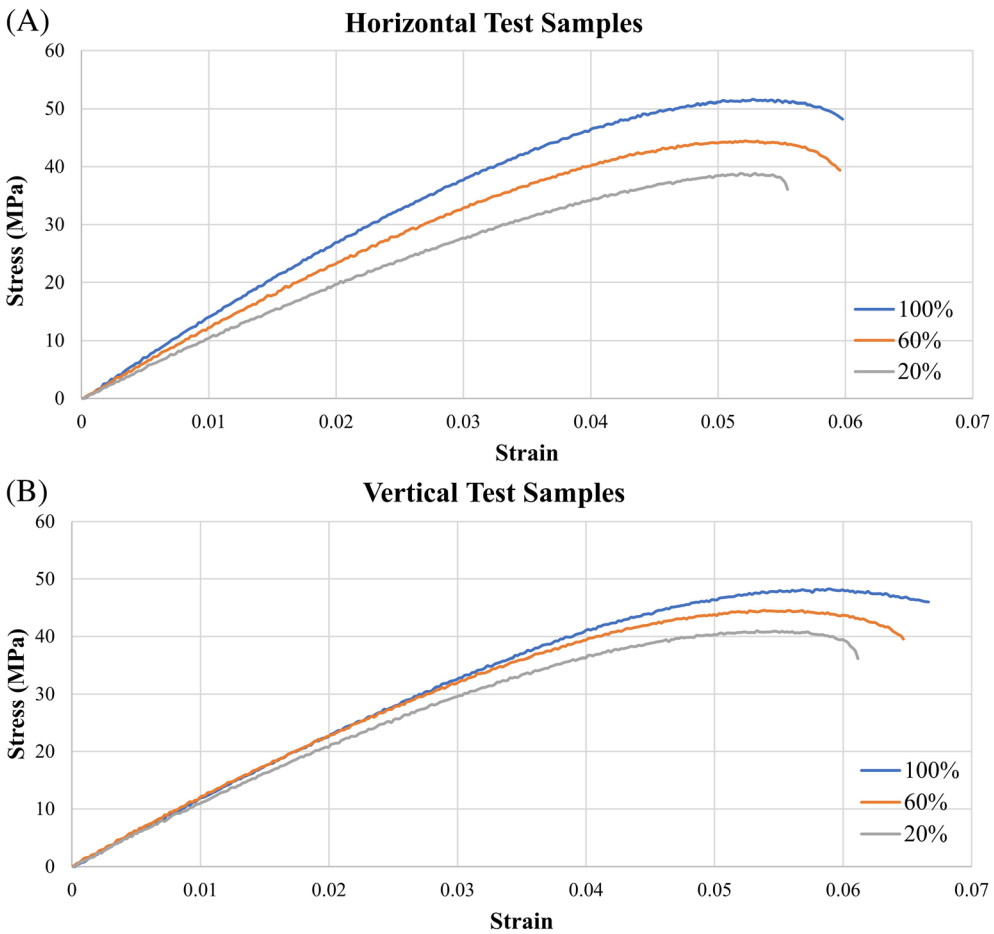

strength and elastic modulus. That kind of trend can be attributed to the rising volume fraction of the load-bearing thermoplastic material. Likewise, Srinivasan et al.[40] also reported that increasing infill density (from 20% to 100%) enhanced the tensile strength values of the FDM-printed standard PET-G materials. As for the effect of the building direction, vertical samples exhibited better performance in terms of the tensile strength than the horizontal samples. The highest value of 51.5 MPa was calculated for the vertically built sample with 100% infill, while the lowest value of 38.8 MPa was detected for the horizontally fabricated sample with 20% infill. The main reason behind this outcome is the layer orientation that aligns longitudinally along the tensile force. Due to the parallel aligned layers, applied tensile loads force the rigid polymer body shaper-induced deformation between the thermoplastic chains, thereby blocking the brittle fracture emerging after the notch effect.

To compare the experimental and numerical vibration results, elastic modulus values of the fabricated samples are required. In this work, experimentally calculated values were used in the simulation efforts, and the same model was used. At this point, all numerical results of the tensile tests were shared in Table 2 in detail with related standard deviation (SD) values.

3.2 | Vibrations results

This study investigated how various design parameters, including beam lengths (150, 175, and 200 mm), infill rates (20%, 60%, and 100%), and building direction (vertical and horizontal), influence the natural frequencies of RePET-G beams. Experimental and numerical analyses were conducted to determine the modal parameters of the RePET-G beams. The experimental studies utilized Dewesoft X data acquisition and signal processing software. For the numerical analyses, ANSYS and DQM were employed, using the mechanical properties specified in Table 2. These values were ascertained by subjecting the test specimens, prepared in compliance with the ASTM D 3039 standard, to testing with a tensile machine. A total of 54 test samples were produced for the vibration tests, with three samples for each configuration. The samples were prepared following ASTM standards and relevant theories from the literature. In the calculations, the data were averaged across all samples. In numerical and experimental analyses, the fixed-free condition was considered the boundary condition.

The scatterplot Figure 8 illustrates the comparison between experimental first natural frequencies and those obtained by the DQM method for the RePET-G beams. The figure depicts the outcomes of the regression analysis, revealing a clear linear correlation between the numerical and experimental approaches. Moreover, the adjusted R^2 values closely approach 1 for each building directions. Consequently, the mathematical determination of the relationship between the numerical and experimental outcomes is evident, demonstrating a high level of compatibility between the results.

Following the determination of the relationship between these methods via linear regression analysis, the effects of printing parameters and geometrical properties on the natural frequencies of the RePET-G beams are shown in Figures 9 and 10. Figure 9 shows the effect of changes in beam length and infill rate on the natural frequencies obtained using numerical and experimental methods for RePET-G beams with vertical building direction. It can be seen from Figure 3 that the natural frequency values obtained from ANSYS, DQM, and experimental methods are highly consistent with each other for each configuration. Additionally, it should be noted that the beam length significantly influences the natural frequencies. Increasing the beam length leads to a decrease in the structure's stiffness, resulting in lower natural frequency values for all configurations of the RePET-G beam. Decreasing the beam length, especially when the working frequency approaches the lowest natural frequency of the structure, will result in widening the disparity between natural and working frequencies, leading to a safer design. When examining the effects of filament infill rates on natural frequencies (Figure 9), it is

TABLE 2 Mechanical properties of recycled polyethylene terephthalate glycol materials according to infill rates and building direction.

	Horizontal			Vertical		
	100%	60%	20%	100%	60%	20%
Elasticity modulus (MPa)	1322.35 (SD: 9.26)	1144.62 (SD: 9.58)	970.26 (SD: 10.72)	1136.82 (SD: 8.76)	1102.07 (SD: 8.98)	1026.93 (SD: 9.32)
Tensile strength (MPa)	51.58 (SD: 2.76)	44.44 (SD: 2.97)	38.84 (SD: 2.91)	48.27 (SD: 2.48)	44.54 (SD: 2.81)	40.99 (SD: 2.76)
Elongation at break (%)	5.98 (SD: 0.07)	5.98 (SD: 0.07)	5.54 (SD: 0.06)	6.66 (SD: 0.08)	6.47 (SD: 0.09)	6.11 (SD: 0.08)

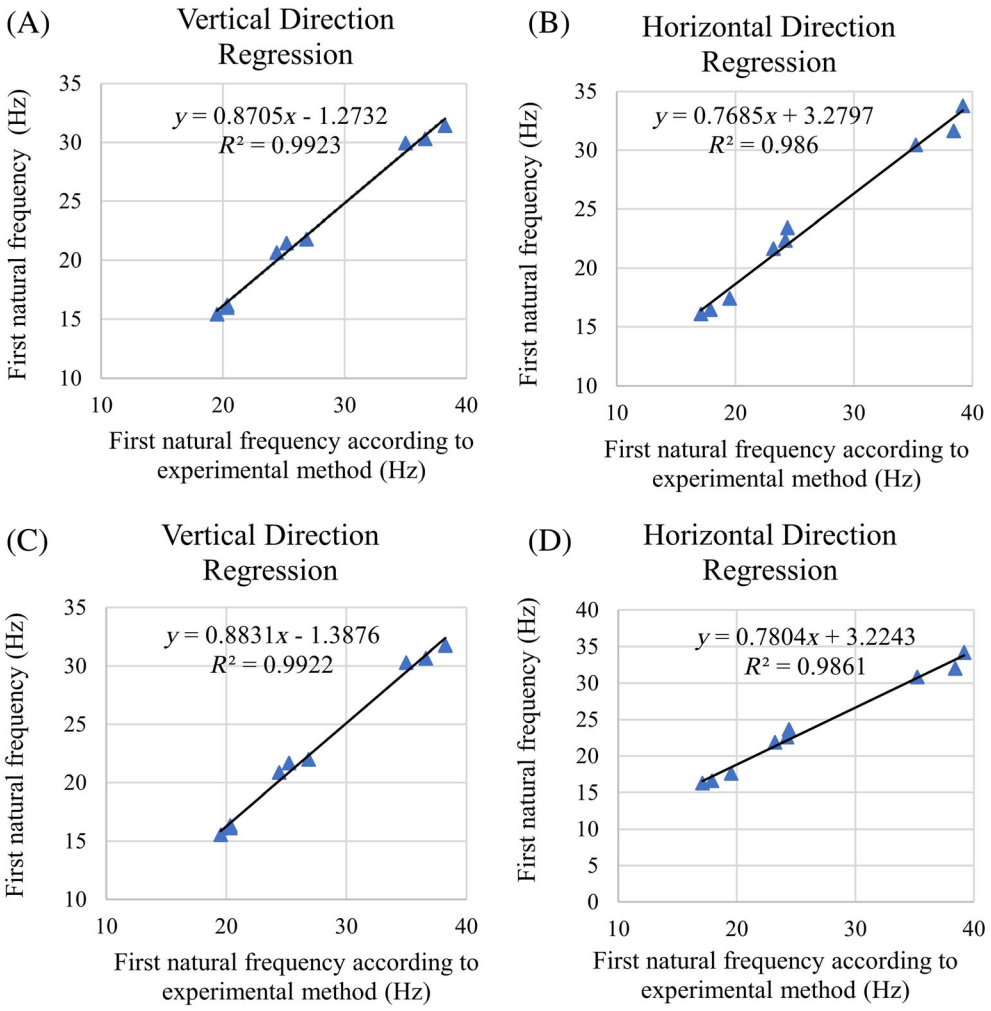

FIGURE 8 The scatterplot displaying the first natural frequency values obtained experimentally versus those acquired by the numerical methods for recycled polyethylene terephthalate glycol beams: (A) differential quadrature method (DQM) versus exp. for vertical direction, (B) DQM versus exp. for horizontal direction, (C) ANSYS versus exp. for vertical direction, and (D) ANSYS versus exp. for horizontal direction.

observed that as the infill rate increases from 20% to 100% for configurations with the same beam length, there is a slight decrease in the natural frequency values of the structure. As the infill rate goes up from 20% to 100%, the stiffness (Table 2) and density (Figure 6) of the structure also ascend. The low impact of changes in infill rates is due to the similar magnitude of changes in stiffness and density of the structure. The study by Parpala et al., investigating the effects of infill rate, number of countours, and infill width on the vibration properties of 3D printed PLA samples with dimensions of 280 mm × 20 mm × 3.6 mm, is supportive of this result. According to the findings of their performance, it can be reported that the first natural frequency of the beam dropped to 100 Hz from 105.7 Hz with the increase of the infill rate from 25% to 50% when the other parameters kept fixed. In addition, a similar trend was obtained in this study too, and for example, with the raise of the infill rate from 20% to 100% for a length of 150 mm, the experimental first natural frequency decreased from 38.25 to 34.99 Hz.

Figure 10 illustrates the impact of variations in beam length and infill rate on the natural frequencies obtained using numerical and experimental methods for RePET-G beams with a horizontal building direction. As shown in Figure 10, the values derived from numerical methods align well with the experimental results, indicating that ANSYS, DQM, and experimental methods yield similar values. This case indicates the production reliability of the applied FFF technology and fabrication repetitiveness that provides similar void structures in the sample bodies. The figure clearly demonstrates that beam length significantly affects the natural frequencies as also happened in the vertical versions. A reduction in beam length increases the natural frequencies of the structure. The decrease in the beam length enhances the structure's stiffness, resulting in higher natural frequency values for all configurations of the RePET-G beam. When considering the effects of filament infill rates on natural frequencies (Figure 10), it is evident that variations in infill rates altered the first natural frequencies slightly, and there was not any apparent rising/decreasing trend in the results depending on the climbing infill rates. Figure 10 shows that as the infill rate increases from 20% to 100% for configurations with

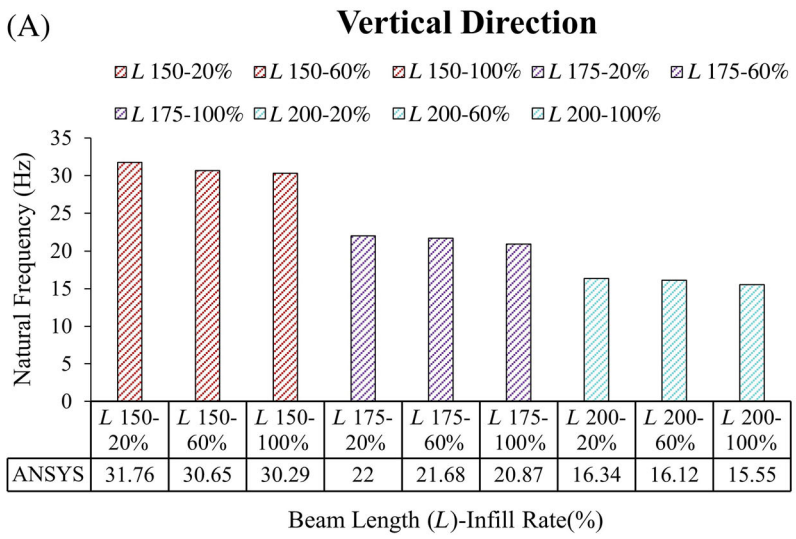

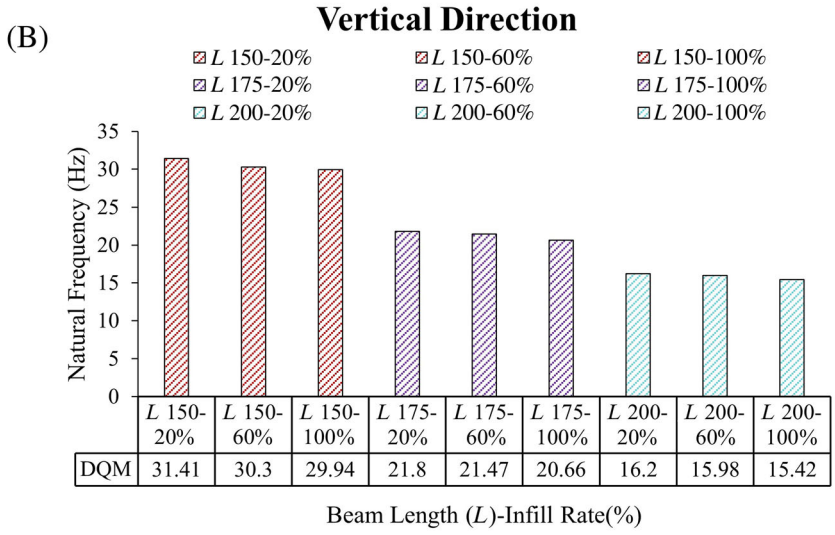

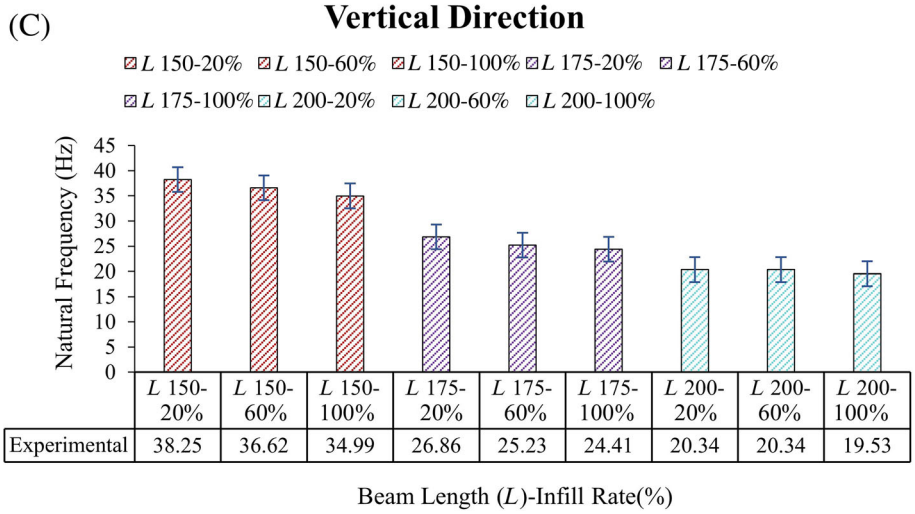

FIGURE 9 The variation of natural frequency values of recycled polyethylene terephthalate glycol beams with vertical building direction based on beam length, infill rate, and solution method: (A) ANSYS, (B) differential quadrature method (DQM), and (C) experimental.

the same beam length, there is an oscillation in the natural frequency values of the structure. This circumstance might be triggered by the micro-scale warpage and relatively wide cross-sectional area of the separation surfaces of the horizontal samples. The minimal impact of changes in infill rates can also be attributed to the similar extent of changes in the structure's stiffness and density.

When Figures 9 and 10 are examined together, the effect of changes in horizontal and vertical building

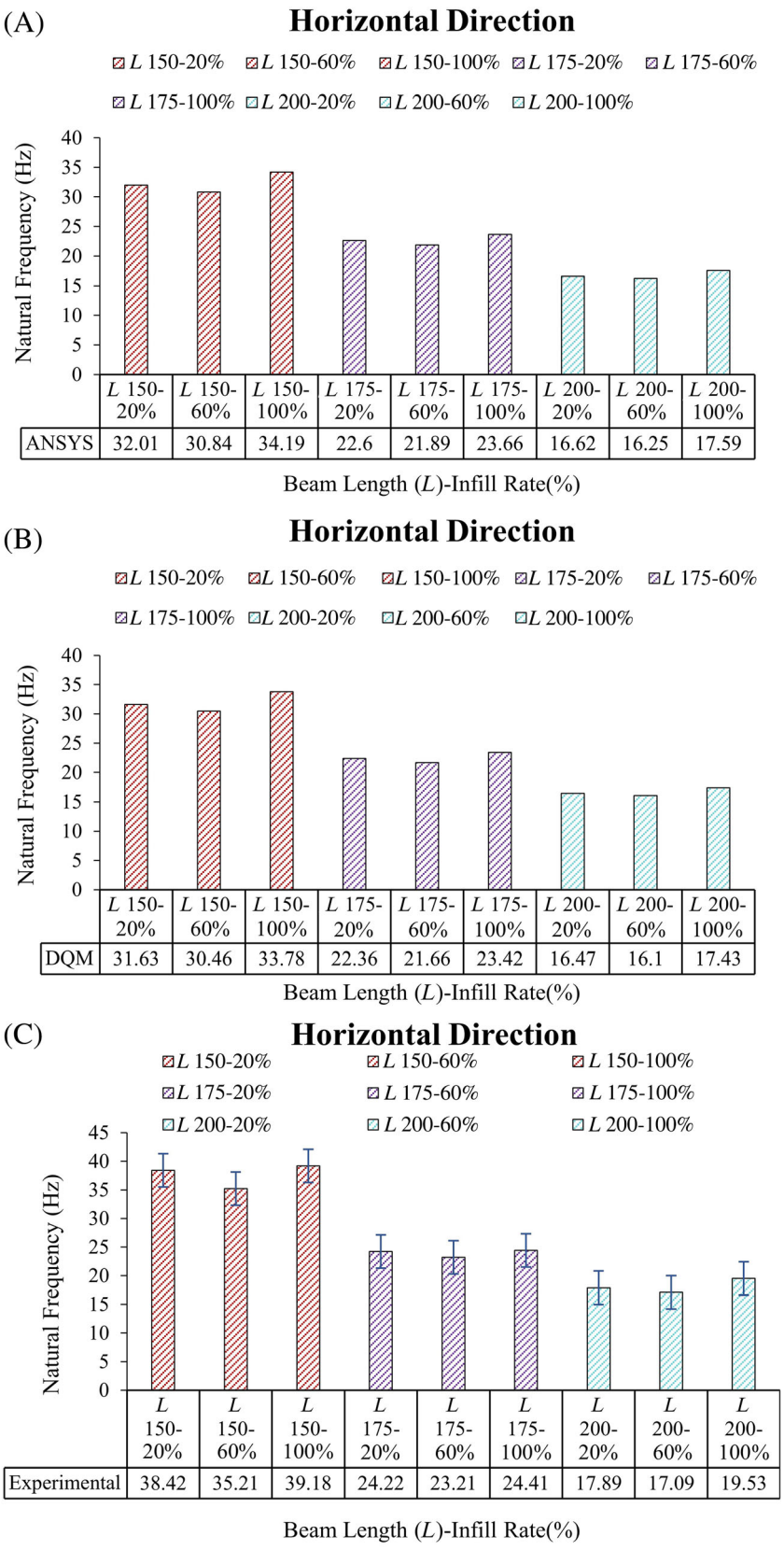

FIGURE 10 The variation of natural frequency values of recycled polyethylene terephthalate glycol beams with horizontal building direction based on beam length, infill rate, and solution method: (A) ANSYS, (B) differential quadrature method (DQM), and (C) experimental.

directions on the natural frequencies obtained using numerical and experimental methods for RePET-G beams with varying beam lengths and infill rates is also seen. However, for beams with the same length and an infill rate of 100%, the natural frequency values obtained from numerical methods in the horizontal building

direction are determined to be higher than those obtained in the vertical building direction. The reason for this is that, in the case of a 100% infill rate, the samples in the horizontal building direction have higher rigidity (Figure 7) and lower density (higher production gaps between the accumulation layers) (Table 2). When the pertinent studies in the literature backing this conclusion are scrutinized, Chaitanya et al.[41] performed a research on the vibrational behavior of 3D-printed ABS beam with a length, width, and thickness of 250, 25, and 5 mm, respectively. In conclusion, they reported that the change of build orientation from flat to vertical, the first natural frequency value of 34.38 Hz was reduced to 31.74 Hz.

Upon reviewing the literature, it became apparent that the obtaining the natural frequency of 3D-printed PET-G beams is rarely explored. Ali and Chowdary[42] examined a study about the influences of raster angle, air gap, build orientation, and number of contours on the natural frequency of 3D printed PC beams with a length of 150 mm, width of 20 mm, and thickness of 4 mm. As a result of their study, they announced that the first natural frequency values ranged between approximately 25 and 45 Hz depending on the variations of the 3D printing parameters. What's more, İyibilgin et al.[43] studied the natural frequency values of 3D printed PLA beams with the dimensions of 700 mm × 20 mm × 10 mm. In this study, the infill patterns of the beams were also varied, such as square, rectangle, triangle, wiggle, honeycomb, and full. Lastly, it was pointed out that the first natural frequency values were found to be between 28 and 32.5 Hz. Furthermore, Ergene et al.[28] carried out the effect of infill rate and layer thickness of 3D printed PET-G beams on their first natural frequency by experimental and numerical analysis, and first natural frequency values were fluctuated between 17.97 and 19.31 Hz for layer thickness of 0.1 mm. According to these valuable efforts, the recycling of the PET-G filaments and the vibration performance of the produced RePET-G components are notably competitive in comparison with the existing 3D-printed polymers reported in the academic archives. With the recycling studies, a cleaner methodology is not only provided, but an efficient natural frequency value can be obtained by way of 3D printing technique.

4 | CONCLUSIONS

The recycling of engineering components and thus achieving low-cost production solutions is extremely important today. In this context, this research experimentally examined the tensile behavior of RePET-G beams. Furthermore, free vibration analysis was performed numerically with the DQM method and ANSYS software and experimentally with a vibration measurement system. Thus, it aimed to contribute to the literature by determining numerically and experimentally the effect of 3D printing parameters (beam length and infill rate) and building direction (vertical and horizontal) on the natural frequency values of 3D-printed RePET-G beams. The following is a summary of the findings and conclusions from the examined configurations.

It is clearly evident that the natural frequency values obtained from numerical methods such as DQM and ANSYS are in good agreement with those obtained experimentally. Regardless of the construction direction and infill rate, when the length of the RePET-G beam increases, the natural frequency decreases. A decrease in stiffness directly causes a decrease in frequency. In configurations with vertical building direction and the same beam length, it is observed that there is a slight decrease in the natural frequency values of the structure as the infill rate increases from 20% to 100%. Changes in infill rates in beams with horizontal building direction slightly affected the first natural frequencies, and that there was no significant increase/decrease in the results due to increasing infill rates. It is understood that that there is no significant change in the natural frequencies of beams of the same length and infill rates of 20% and 60% due to changes in building directions. However, for beams of the same length and infill rate of 100%, it is further demonstrated that the natural frequency values obtained from numerical methods in the horizontal building direction are higher than those obtained in the vertical building direction. This research demonstrates a unique showcase of the advantages of the DQM compared to previous studies on the vibration analysis of RePET-G beams.

ACKNOWLEDGMENTS

The authors would like to thank Porima Polymer Technology A.Ş. (Yalova, Türkiye) for the prompt delivery of the RePET-G filaments.

CONFLICT OF INTEREST STATEMENT

The authors state no conflict of interest.

DATA AVAILABILITY STATEMENT

The data that support the findings of this study are available on request from the corresponding author.

ORCID

Çağın Bolat https://orcid.org/0000-0002-4356-4696
Abdulkadir Çebi https://orcid.org/0000-0002-3074-6554

REFERENCES

1. Yang Y, Dai X, Yang B, et al. Optimization of polylactic acid 3D printing parameters based on support vector regression and cuckoo search. *Polym Eng Sci*. 2023;63:3243-3253.

2. Bedi SS, Mallesha V, Mahesh V, et al. Thermal characterization of 3D printable multifunctional graphene-reinforced polyethylene terephthalate glycol (PETG) composite filaments enabled for smart structural applications. *Polym Eng Sci*. 2023;63:2841-2856.
3. Popescu D, Zapciu A, Amza C, Baciu F, Marinescu R. FDM process parameters influence over the mechanical properties of polymer specimens: a review. *Polym Test*. 2018;69:157-166.
4. Liu Z, Wang Y, Wu B, Cui C, Guo Y, Yan C. A critical review of fused deposition modeling 3D printing technology in manufacturing polylactic acid parts. *Int J Adv Manuf Technol*. 2019;102:2877-2889.
5. Chacón JM, Caminero MA, García-Plaza E, Núñez PJ. Additive manufacturing of PLA structures using fused deposition modelling: effect of process parameters on mechanical properties and their optimal selection. *Mater Des*. 2017;124:143-157.
6. Torrado AR, Roberson DA. Failure analysis and anisotropy evaluation of 3D-printed tensile test specimens of different geometries and print raster patterns. *J Fail Anal Prev*. 2016;16:154-164.
7. Parandoush P, Lin D. A review on additive manufacturing of polymer-fiber composites. *Compos Struct*. 2017;182:36-53.
8. Srinivasan R, Prathap P, Raj A, Aswinth Kannan S, Deepak V. Influence of fused deposition modeling process parameters on the mechanical properties of PETG parts. *Mater Today Proc*. 2020;27:1877-1883.
9. Durgashyam K, Indra Reddy M, Balakrishna A, Satyanarayana K. Experimental investigation on mechanical properties of PETG material processed by fused deposition modeling method. *Mater Today Proc*. 2019;18:2052-2059.
10. Szykiedans K, Credo W, Osiński D. Selected mechanical properties of PETG 3-D prints. *Procedia Eng*. 2017;177:455-461.
11. Ajay Kumar M, Khan MS, Mishra SB. Effect of machine parameters on strength and hardness of FDM printed carbon fiber reinforced PETG thermoplastics. *Mater Today Proc*. 2020;27:975-983.
12. Kam M, Saruhan H, İpekçi A. Investigation the effects of 3D printer system vibrations on mechanical properties of the printed products. *Sigma J Eng Nat Sci*. 2018;36:655-666.
13. Singh KV, Khan F, Veta J, Singh AK. Influence of printing orientation on the dynamic characteristics and vibration behavior of 3D printed structures. *ASME 2017 International Design Engineering Technical Conferences and Computers and Information in Engineering Conference, Cleveland, Ohio, 6–9 August*. ASME; 2017. doi:10.1115/DETC2017-68289
14. Wang R, Shang J, Li X, Luo Z, Wu W. Vibration and damping characteristics of 3D printed Kagome lattice with viscoelastic material filling. *Sci Rep*. 2018;8:9604.
15. Lesage P, Dembinski L, Lachat R, Roth S. Mechanical characterization of 3D printed samples under vibration: effect of printing orientation and comparison with subtractive manufacturing. *Results Eng*. 2022;13:100372.
16. Tekes A. 3D-printed torsional mechanism demonstrating fundamentals of free vibrations. *Can J Phys*. 2020;99:125-131.
17. Zolfagharian A, Bodaghi M, Hamzehei R, Parr L, Fard M, Rolfe BF. 3D-printed programmable mechanical metamaterials for vibration isolation and buckling control. *Sustainability*. 2022;14:6831. doi:10.3390/su14116831
18. Zou X, Zeng L, Gu F, et al. An investigation of the vibration responses in a 3D printing process for online condition monitoring BT - proceedings of IncoME-V & CEPE Net-2020. In: Wang D, Wang T, et al., eds. *Zhen D*. Springer International Publishing; 2021:335-344.
19. Kam M, Saruhan H, İpekçi A. Experimental investigation of vibration damping capabilities of 3D printed metal/polymer composite sleeve bearings. *J Thermoplast Compos Mater*. 2022;36:2505-2522.
20. Zhang X, Zhou H, Shi W, Zeng F, Zeng H, Chen G. Vibration tests of 3D printed satellite structure made of lattice sandwich panels. *AIAA J*. 2018;56:4213-4217.
21. Guo Z, Hu G, Jiang J, Yu L, Li X, Liang J. Theoretical and experimental study of the vibration dynamics of a 3D-printed sandwich beam with an hourglass lattice truss core. *Front Mech Eng*. 2021;7. doi:10.3389/fmech.2021.651998
22. Parpala RC, Popescu D, Pupaza C. Infill parameters influence over the natural frequencies of ABS specimens obtained by extrusion-based 3D printing. *Rapid Prototyp J*. 2021;27:1273-1285.
23. Gunasegeran M, Edwin SP. Free and forced vibration analysis of 3D printed bioinspired sandwich beam using HSDT: numerical and experimental study. *Polym Compos*. 2022;43:3659-3677.
24. Medel F, Abad J, Esteban V. Stiffness and damping behavior of 3D printed specimens. *Polym Test*. 2022;109:107529.
25. Mizukami K, Kumamoto Y. 3D printing of fiber composite sandwich metamaterial with spiral resonators for attenuation of low-frequency structural vibration. *Compos Part A Appl Sci Manuf*. 2023;172:107594.
26. Monkova K, Vasina M, Zaludek M, Monka PP, Tkac J. Mechanical vibration damping and compression properties of a lattice structure. *Materials*. 2021;14:1502. doi:10.3390/ma14061502
27. Carter J, Singh KV, Khan F. Vibration characteristics of 3D printed viscoelastic graded polymeric plates. *ASME 2021 International Design Engineering Technical Conferences and Computers and Information in Engineering Conference, 17–19 August*. ASME; 2021. doi:10.1115/DETC2021-68460
28. Ergene B, Atlıhan G, Pinar AM. Experimental and finite element analyses on the vibration behavior of 3D-printed PET-G tapered beams with fused filament fabrication. *Multidiscip Model Mater Struct*. 2023;19:634-651.
29. Carter JB. *Vibration and Aeroelastic Prediction of Multi-material Structures Based on 3D-printed Viscoelastic Polymers*. Miami University. https://www.proquest.com/dissertations-theses/vibration-aeroelastic-prediction-multi-material/docview/2856277376/se-2?accountid=200257 2021.
30. Mahesh V. Experimental investigation on the dynamic response of additive manufactured PETG composite beams reinforced with organically modified montmorillonite nanoclay and short carbon fiber. *Polym Compos*. 2021;42:5021-5034.
31. Mansour M, Tsongas K, Tzetzis D, Antoniadis A. Mechanical and dynamic behavior of fused filament fabrication 3D printed polyethylene terephthalate glycol reinforced with carbon fibers. *Polym Plast Technol Eng*. 2018;57:1715-1725.
32. Kannan S, Manapaya A, Selvaraj R. Frequency and deflection responses of 3D-printed carbon fiber reinforced polylactic acid composites: theoretical and experimental verification. *Polym Compos*. 2023;44:4095-4108.
33. Xue F, Robin G, Boudaoud H, Sanchez FAC, Daya EM. Effect of process parameters on the vibration properties of PLA

structure fabricated by additive manufacturing. *Solid Freeform Fabrication 2021: Proceedings of the 32nd Annual International Solid Freeform Fabrication Symposium, 2–4 August*. University of Texas at Austin; 2021:521-533.
34. Senthamaraikannan C, ParthaaSarathy B, Surya S, Tharun Rajan S. Study on the free vibration analysis and mechanical behaviour of 3D printed composite I shaped beams made up of short carbon fiber reinforced ABS and PLA materials. *Mater Today Proc*. 2023. doi:10.1016/j.matpr.2023.07.141
35. Civalek Ö. Application of differential quadrature (DQ) and harmonic differential quadrature (HDQ) for buckling analysis of thin isotropic plates and elastic columns. *Eng Struct*. 2004;26:171-186.
36. Bellman R, Casti J. Differential quadrature and long-term integration. *J Math Anal Appl*. 1971;34:235-238.
37. Du H, Lim MK, Lin RM. Application of generalized differential quadrature to vibration analysis. *J Sound Vib*. 1995;181:279-293.
38. Ansys. *ANSYS 18.1 Reference Manual*. 2018. Accessed March 10, 2024. https://archive.org/details/ANSYSFluentUsersGuide/mode/2up
39. Ergene B, Bolat Ç. An experimental study on the role of manufacturing parameters on the dry sliding wear performance of additively manufactured PETG. *Int Polym Process*. 2022;37:255-270.
40. Srinivasan R, Ruban W, Deepanraj A, Bhuvanesh R, Bhuvanesh T. Effect on infill density on mechanical properties of PETG part fabricated by fused deposition modelling. *Mater Today Proc*. 2020;27:1838-1842.
41. Chaitanya SK, Reddy K, Ch SNSH. Vibration properties of 3D printed/rapid prototype parts. *Int J Innov Res Sci Eng Technol*. 2015;3297:4602.
42. Ali F, Chowdary BV. Natural frequency prediction of FDM manufactured parts using ANN approach. *IFAC-PapersOnLine*. 2019;52:403-408.
43. İyibilgin O, Dal H, Gepek E. Experimental modal analysis of 3D printed beams. *4th International Congress on 3D Printing (Additive Manufacturing) Technologies and Digital Industry, Antalya, Turkey, 11–14 April*; 2019:613-620.

SUPPORTING INFORMATION

Additional supporting information can be found online in the Supporting Information section at the end of this article.

How to cite this article: Bolat Ç, Çebi A, Maraş S, Ergene B. An experimental and numerical effort on the vibration behavior of additively manufactured recycled polyethylene terephthalate glycol components. *Polym Eng Sci*. 2024;1-16. doi:10.1002/pen.26954